Chinese Chemical Letters 35 (2024) 109014

Contents lists available at ScienceDirect

Chinese Chemical Letters

journal homepage: www.elsevier.com/locate/cclet

Doping-induced charge transfer in conductive polymers

Siyi Luo[a,b], Zhen Xu[a,b], Fei Zhong[a,b], Hui Li[a,*], Lidong Chen[a,b]

[a] State Key Laboratory of High Performance Ceramics and Superfine Microstructures, Shanghai Institute of Ceramics, Chinese Academy of Sciences, Shanghai 200050, China

[b] Center of Materials Science and Optoelectronics Engineering, University of Chinese Academy of Sciences, Beijing 100049, China

ARTICLE INFO

Article history:
Received 7 June 2023
Revised 27 August 2023
Accepted 28 August 2023
Available online 1 September 2023

Keywords:
Molecular doping
Charge transfer
Integer charge transfer
Charge transfer complex
Conjugated polymer

ABSTRACT

Molecular doping has become a widely used method to modulate the electric performance of organic semiconductors (OSC). Highly effective charge transfer during molecular doping is desired to achieve ideal electrical conductivity. Two types of charge transfer mechanisms are widely accepted in molecular doping process: integer charge transfer (ICT) and charge transfer complex (CTC). In this review, fundamental principles of two mechanisms are revisited and the characterization methods are depicted. The key points for the formation of two mechanisms are highlighted from aspects of molecular structure and process engineering. Then, the strategies to improve the proportion of ICT are discussed. Finally, the challenges and perspectives for future developments in the molecular doping of polymer semiconductors are provided.

1. Introduction

Organic semiconductors (OSC), especially conjugated polymers, have shown promising application in organic optoelectronic and energy-conversion devices [1,2], such as organic light-emitting diodes, thin-film transistors, solar cells, and thermoelectric devices, owing to the advantages of low-cost production, solution processibility and flexibility. Pristine OSCs have low intrinsic electrical conductivities. It is essential to improve the electrical performance by the chemical doping process. In the 1970s, phthalocyanine and polyacetylene were successfully doped by exposure to halogen vapors [3,4]. The electrical conductivity can be increased by several orders of magnitude [5]. Nevertheless, a strong tendency to diffuse of the halide happens, which strongly impairs both the device performance and the operation lifetime. To achieve precise and controllable doping, molecular doping of OSC, by using a small organic molecule with a conjugated backbone as an acceptor, has been widely used to control the fermi level of OSC [6–10] and the contact resistance between interfaces [11–16] in electronic devices. So far, an in-depth understanding of the interaction between OSC and dopant to achieve effective doping is still desired.

The low doping efficiency of molecular doping for OSC is a big limitation to pursuing the high electrical conductivity. To improve the doping efficiency, the traditional methods prefer to increase the dopant concentration. However, the excess of dopants destroys the crystal structure of organic semiconductor and introduces traps and scattering sites [17,18]. As a result, the carrier mobility of doped film will be decreased, and thus the electrical conductivity is damaged. To avoid disrupting the packing of semiconductor upon doping, new doping strategies, such as sequential doping [19–24], ion-exchange doping [25], and hybrid doping [26], have been recently developed. On the other hand, the doping mechanism remains controversial compared with the inorganic counterparts [27]. The simplified understanding about doping is the charge transfer between a semiconductor and a given dopant forced by the energy level difference [28–30]. For example, poly(3-hexylthiophene) (P3HT), with an ionization potential (IP) about 5.0 eV, is matched with 2,3,5,6-tetrafluoro-7,7,8,8-tetracyanoquinodimethane (F4TCNQ) with an electron affinity (EA) about 5.2 eV, so the electron transfer between P3HT and dopant is spontaneous. By now, two types of charge transfer mechanisms are widely accepted (for p-type doping): (1) integer charge transfer (ICT) to form isolated hole and dopant anion; (2) partial charge transfer to form charge transfer complex (CTC). ICT refers to the complete charge transfer of an electron between an organic semiconductor and a dopant, while the hybridization of organic semiconductor and dopants exists in CTC. In general, the formation of ICT is beneficial to improve the carrier concentration and consequently increase the electrical conductivity. On the contrary, CTC cannot contribute substantially to the carrier concentration due to the charge localization.

This review will highlight the mechanism of charge transfer, with particular focus on the p-type organic semiconductor doped by F4TCNQ. We will introduce the key factors determining the

* Corresponding author.
E-mail address: lihui889@mail.sic.ac.cn (H. Li).

https://doi.org/10.1016/j.cclet.2023.109014
1001-8417/

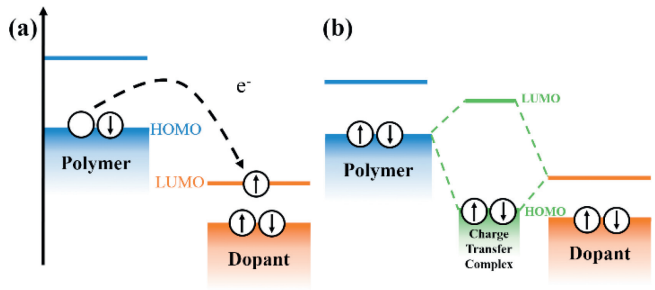

Fig. 1. Basic concept map of (a) ICT and (b) CTC between p-type polymers and dopants.

charge transfer degree, and then discuss the strategies to improve the proportion of ICT through materials design principles and doping techniques as well as future challenges for molecular doping of polymer semiconductors.

2. The degree of charge transfer in OSC

For p-type doping, ICT process means an electron can be completely extracted by the dopant acceptor from the conjugated polymer [28], accompanying the generation of a hole on the polymer backbone and a dopant anion (Fig. 1a). For n-type doping, an electron transfers occurs from dopants' highest occupied molecular orbital (HOMO) to polymer's lowest unoccupied molecular orbital (LUMO), which leads to the formation of an electron on the polymer backbone and a dopant cation. It has been demonstrated that the ICT process consists of two steps: charge transfer from donor to acceptor and subsequent dissociation of integer-charge transfer complex [31]. The first step is dominated by the difference between HOMO level of donor and LUMO level of acceptor. This step is negligibly temperature-activated. The second step is controlled by the thermal activation which is related to the electrostatic interaction and the local energetic disorder accompanying with broadened density of states (DOS) and reduced activation energy. The CTC model was observed in F4TCNQ doped pentaphene [32–34]. For CTC, the frontier molecular orbitals of dopant and polymer semiconductor are hybridized to form new occupied bonding orbitals and unoccupied antibonding orbitals (Fig. 1b) [35]. The electron donor (semiconductor) and the acceptor (dopant) are attracted by electrostatic interaction and keep electrically neutral as a unity. Electrons can sometimes be excited from the HOMO of the semiconductor to the antibonding state in hybrid state, leaving behind a hole on polymer backbone by the thermal excitation. In Hückle model [36–38], the energy level of molecular orbitals of CTC in p-type doping can be expressed as follows (Eq. 1):

$$E_{\mathrm{CTC,H/L}} = \frac{H_{\mathrm{poly}} + L_{\mathrm{dop}}}{2} \pm \sqrt{\left(H_{\mathrm{poly}} - L_{\mathrm{dop}}\right)^2 + 4\beta^2} \quad (1)$$

where, H_{poly} and L_{dop} denote the HOMO level of polymer and the LUMO level of dopant; and β is a resonance integral based on intermolecular coupling between polymer and dopant. According to this equation, only increasing the p-dopant EA is not sufficient to achieve higher doping efficiency. The additional criterion is reducing the intermolecular resonance integral β.

The charge transfer degree can be characterized and analyzed by UV-vis-NIR and Fourier transform infrared spectrometer (FTIR). As shown in Fig. 2, the absorption peaks of dopant anion peak (410 nm, 765 nm and 870 nm) and (bi)polarons (1400-2000 nm) in infrared region can be observed in UV-vis-NIR spectra of F4TCNQ doped P3HT film, which represents the formation of ICT [39–41]. FTIR spectra can be employed to distinguish the degree of charge transfer (δ) by characterizing the C≡N vibrational peak of F4TCNQ [42]. According to Mulliken's theory [43], δ can be calculated by the following equation (Eq. 2):

$$\delta = \frac{2\Delta\nu}{\nu_0}\left(1 - \frac{\nu_1^2}{\nu_0^2}\right)^{-1} \quad (2)$$

where, ν_0 is the wavenumber of the neutral F4TCNQ, ν_1 is the wavenumber of the F4TCNQ anion, and $\Delta\nu$ is the difference value of wavenumber of the actual peak and the neutral F4TCNQ. The C≡N vibrational peak appearing in 2194 cm^{-1} endows $\delta = 1$, indicates the existence of F4TCNQ anion, while the vibrational peak in 2207 cm^{-1} ($\delta = 0.6$) means the appearance of CTC (Fig. 2b).

For a doped conjugated polymer, it is more likely to form ICT than CTC with the dopants tending to insert into the side chains spaces along the lamellar direction theoretically. Experimentally, both ICT and CTC can be detected in a doped polymer. For example, both integer and partial charge transfer peaks appear in the FTIR spectra of F4TCNQ doped P3HT or poly(2,5-bis(3-tetradecylthiophen-2-yl)thieno[3,2-*b*]thiophene) PBTTT film [44–46]. In the process of ICT, the dopants being far from the polymer backbone results in the negligible disruption of polymer crystal structure and π-stacking in this microstructure (Fig. 3a) [35,45,47]. It was found that the dopants still prefer to reside in the lamellar region even if its size is larger than polymer lamellar spacing [48]. For example, dodecaborane (DDB) based dopant with size of 2 nm is larger than the lamellar distance of P3HT. The dopant prefers to insert into the lamellar structure and form ICT. However, the branched side chains of P3EHT may force the dopant F4TCNQ to insert into the π-π stacking, leading to a charge transfer complex [49]. Stanfield *et al.* reported that thermal annealing could convert CTC to ICT [50], indicating that the CTC phase is not thermodynamically preferred. The molecular dynamics simulation of

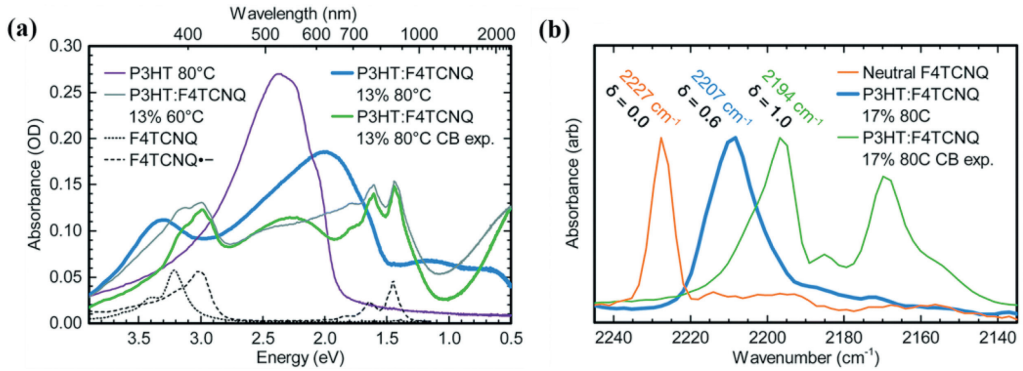

Fig. 2. (a) The UV-vis-NIR of F4TCNQ doped P3HT and (b) FTIR of the C≡N vibrational peak of neutral F4TCNQ and F4TCNQ anion in F4TCNQ doped P3HT. Copied with permission [41]. Copyright 2018, the Royal Society of Chemistry.

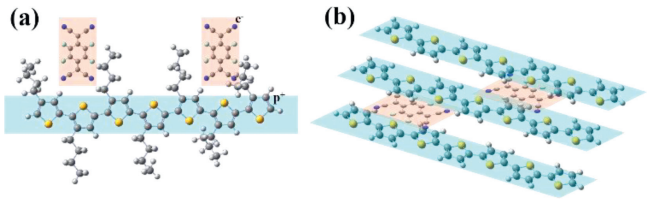

Fig. 3. (a) The dopant F4TCNQ prefers to insert into the side chains of polymer in ICT. (b) The dopant F4TCNQ is coplanar with polymer backbone in CTC.

F4TCNQ doped P3HT shows that the barrier energy for insertion of a dopant molecular into polymer is lower for formation of ICT than that for CTC. Besides, density functional theory (DFT) calculation implies that ICT is the thermodynamically preferred in conjugated polymer because the entropic cost of forming ICT is positive, while it is negative for CTC [51]. Moreover, the process of CTC is infrequent in doped polymers, as it needs change on the configuration or microstructure. For example, the distance between π-π stacking and lamellar space of polymer decrease with the increase of CTC proportion. Combining X-ray absorption near edge structure (XANES) analysis and DFT calculation, several local conformations of CTCs in F4TCNQ doped P3HT was observed. The dominant conformation of F4TCNQ was no longer a planar configuration but the C≡N bents to the polymer backbone due to the electron contribution of P3HT [52].

Experimentally, CTC is preferentially observed in organic small molecules [53]. Different from the microstructure of ICT, the dopants insert into the π-stacking of host molecule backbone. Therefore, π-π interaction occurs between dopants and the host molecule in CTC (Fig. 3b). Several reports have shown that CTC is beneficial to form ordered microstructure and even crystals [40,41,45]. It is found that when CTC occurs in F4TCNQ doped quaterthiophene (4T), a new crystalline phase will be formed in which 4T and F4TCNQ show a coplanar π-stacking, with a fishbone arrangement [54]. In addition, the face-to-face conformation in CTC makes the change in length of carbon-carbon bonds along the backbones of CTC in oligomer less than ICT, by calculating PCPDT-BT's oligomers with different lengths doped by three different dopants [55]. Interestingly, CTCs are thought to induce J-type aggregation and thus contribute to the generation of ICT [56].

3. Effect of charge transfer degree on electrical properties

Obviously, the electrical conductivity ($\sigma = ne\mu$) of the doped semiconductors is intimately related to the process of charge transfer, because only the free carriers can contribute to the carrier concentration (n) and the microstructures of charge-transfer species have a remarkable influence on the carrier mobility (μ) [57]. Several studies have demonstrated that the conductivity of films with ICT species is much higher than those films with CTC species, as the former ones generate abundant (bi)polarons and have less disruption to the microstructure [40,50]. For instance, Pingel *et al.* found that over a half of dopant molecules were ionized to form ICT in F4TCNQ doped P3HT [28]. Although only 5% of charge carrier pairs are totally dissociated into free carriers and contribute to the charge transport due to the low dielectric constant of P3HT, the conductivity can be increased by 2-3 orders of magnitude due to the generation of ICT [41]. Most of carriers are localized due to Coulombic interactions between polymer chains and dopant anions in the p-type doping process [29,58]. Increasing the difference between the HOMO level of polymers and the LUMO level of dopants is an efficient way to improve the conductivity, as the difference is the driving force for charge transfer [59]. For example, the HOMO level of PBDTDTBTF-1, PBDTDTBTF-2, and PBDTDTBTF-3 is -5.33, -5.37, and -5.41 eV, respectively. As a result, the conductivity of PBDTDTBTF-1 is higher than that of PBDTDTBTF-2 and PBDTDTBTF-3 if doped by the same dopant [60].

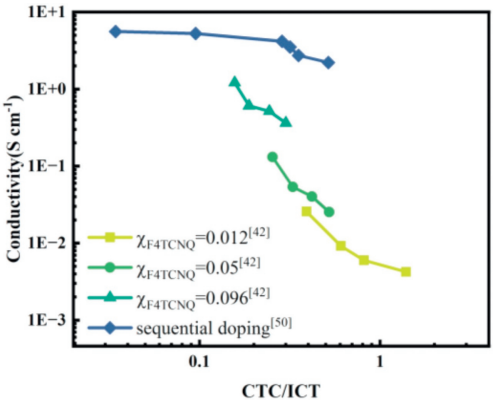

Fig. 4. The relationship between the proportion of CTC/ICT and conductivity in F4TCNQ doped P3HT. Reproduced with permission [42]. Copyright 2019, American Chemical Society. Reproduced with permission [50]. Copyright 2021, American Chemical Society.

Since the energy of hybrid orbitals in CTC is several tens of eV which is much higher than the ionization potential of polymer, only a small fraction of CTC can be ionized, resulting in a low doping efficiency [61]. Therefore, carriers in CTC are localized and bound to the complexes so that they scarcely contribute to the conductivity [41,50]. Nevertheless, P3HT film doped by F4TCNQ vapor shows an order of magnitude higher conductivity than that of solution-doped film, which can be ascribed to the fact that dopants enter into the side chain region to generate ICT with less disruption to the original microstructure [13,51].

The conductivity of F4TCNQ doped P3HT with the varied ratio of CTC/ICT by altering doping time or doping method is summarized in Fig. 4. The ratio of CTC/ICT is obtained from the peak area proportion in the FTIR. Under the same doping concentration, the conductivity shows a downward trend with the increase of CTC content, by blending doping [42] or sequential doping [50] method. The decrease in conductivity is attributed to the reduction of carrier concentration caused by the generation of CTCs [62]. Therefore, great efforts have been given to get complete ICT rather than CTC to pursue the high conductivity. Recently, it has been demonstrated that the existence of CTC is beneficial to charge transport. CTC species in amorphous regions in the film can act as bridges for carrier migration [16,50] to improve the carrier mobility and stabilize the electrical performance. For example, F4TCNQ doped PBTTT film with a moderate (~33%) proportion of CTC does not show any degradation of conductivity for 60 min at 100 °C, while the film containing a low proportion of CTC exhibits a dramatically reduced conductivity. Ratcliff *et al.* have reported that ICT can be transferred into CTC due to the lower stability of the former one under inert dark conditions or dark ambient environment, and thus conductivity obviously decreases [42]. Generally, the formation of ICT is more desired for the improvement of electrical performance than the generation of CTC. Therefore, efforts to achieve the increase of the proportion of ICT are still required.

4. Strategies for complete charge transfer

The main factors determining the degree of charge transfer are the chemical structure (energy level) and film microstructure. To achieve complete charge transfer in doped polymers, effective strategies *via* polymer structure modification, microstructure optimization and ion-exchange doping have been proposed.

4.1. Structure design to control the degree of the charge transfer

The energy level of polymers can be controlled by structure design, including backbone modification and side chain engineering. Thus, the driving force for charge transfer between polymer and dopant can be adjusted to improve the doping efficiency and control the proportion of ICT and CTC. David *et al.* have found that the larger the discrepancy between the HOMO of donor and the LUMO of acceptor, the higher possibility of complete charge transfer. Even double doping (two charges can transfer) can be achieved by further raising the HOMO level [63]. For example, the energy difference between P(a2T-TT) (-4.9 eV) and F4TCNQ (-5.2 eV) is only enough to transfer one electron while the HOMO level of P($g_4$2T-TT) (-4.5 eV) is higher enough to transfer two electrons to F4TCNQ, leading to a doping efficiency reaching 172%. Moreover, the substitution of Se for S in thiophene can slightly increase the HOMO level owing to the large overlap between Se and conjugated backbones. Introducing the electron-donating groups to side chains, such as amino, alkoxy, hydroxy group, is another strategy to raise the HOMO level. For example, the HOMO levels of $Pg_3$2T-TT, $Pg_3$2T-OTz and P2TS-OTz are -4.46 eV, -4.65 eV, and -5.13 eV, respectively, due to the existence of the alkoxy side chains in $Pg_3$2T-TT, $Pg_3$2T-OTz. The degree of charge transfer of three polymers gradually decreases when doped by F4TCNQ and CTC occurs in P2TS-OTz. Moreover, the insertion of one S or O atom in the side chain can also raise the HOMO level. For instance, the HOMO level of PBTTT-^{8}O (-4.95 eV) is slightly higher than that of PBTTT-C_{12} (-5.10 eV). Thus, a stronger polymer-dopant interaction and a higher doping efficiency is obtained in the former one doped by hexafluoro-tetracyanonaphthoquinodimethane (F6TCNNQ) [64].

Besides the direct effect on energy level of polymers, structure design can also affect the interaction between polymer and dopant and then influence the degree of charge transfer. Due to the presence of the delocalized π electron, conjugated polymer typically with a rigid backbone and a planar structure facilitates intense staking and the formation of crystal domains. It was discovered that higher content of ICT can be obtained by replacing S atom in thiophene with Se or Te. The low rotational degrees of selenophene or tellurophene backbone prevents the intercalation of F4TCNQ in π-stacking of polymer [40]. The structure of side chain not only influences the solubility of polymers [65]. Besides, the side chain modulation, including the length, branched or linear, the density along the backbone, plays an important role in microstructure [66]. Comin *et al.* found that polymers with linear alkyl chain tend to create ICT and generate high conductivity, as shown in Fig. 5 [44]. However, it is easier to form CTCs rather than ICT for branch alkyl side chains, due to the steric hindrance of bulky side chains. For example, compared with F4TCNQ doped P3HT film in which F4TCNQ inserts into the side chains, the coplanar π-π stacking is formed in F4TCNQ doped poly(3-(2′-ethyl)hexylthiophene) (P3EHT) [49]. To verify the synergistic effect of backbone and side chain on the degree of charge transfer, our group designed a series of polymers, such as $Pg_3$2T-OTz, PB2T-OTz, P2T-OTz, and P2TS-OTz (Fig. 6) [16]. It is demonstrated that copolymerization of weak acceptor and strong donor combined with nonpolar (alkoxy) and polar (ethylene glycol) side chain can effectively improve conductivity to 550 S/cm because of ICT formation *via* the dopants inserting in side chains region, while CTC act as a charge transport bridge in amorphous region. In addition, the packing of polymer $Pg_3$2T-OTz transfers from face-on to edge-on orientation to form ordered microstructure so that carrier concentration and mobility are simultaneously improved.

The molecular weight related to the number of the repeat units is also an important factor to affect the degree of charge transfer. Liu *et al.* have systematically studied the charge transfer behavior of different length of oligothiophenes and found that the fraction

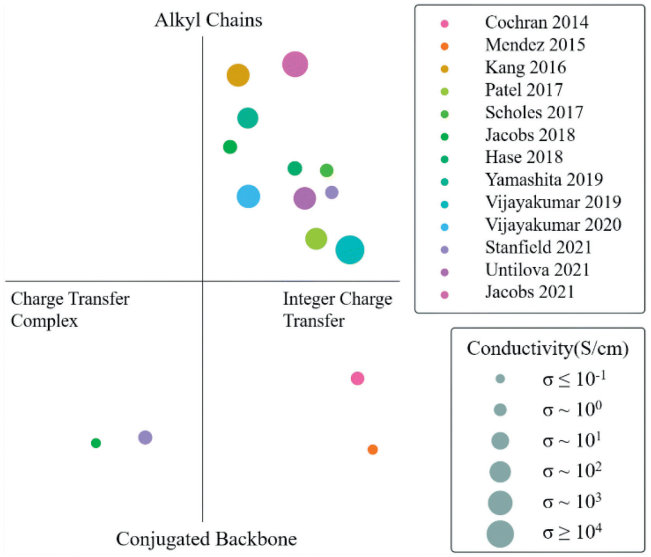

Fig. 5. The relationship between linear alkyl side chain, charge transfer mechanism and conductivity based on available experimental data for PBTTT and P3HT. Copied with permission [44]. Copyright 2022, the Royal Society of Chemistry.

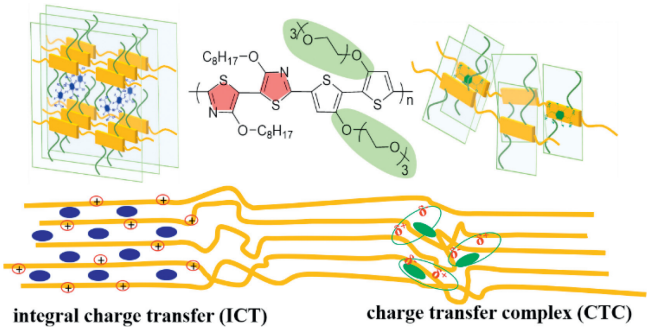

Fig. 6. Schematic illustration of charge transfer in F4TCNQ doped $Pg_3$2T-OTz film. Reproduced with permission [16]. Copyright 2021, Wiley-VCH GmbH.

of ICT increases with the length of oligothiophenes. And the oligothiophene critical length for ICT is suggested to be 10 thiophene units [42,67].

Besides, it has been accepted that the structure of dopants is also a critical factor to affect the degree of charge transfer. The LUMO level of dopant related to its structure affects the driving force of charge transfer [43,54] and the size of dopants also influence the microstructure of film. Coulomb interaction between polymer and dopant plays an important role in carrier dissociation. For example, the polaron concentration in P3HT doped by F4TCNQ is larger than that of doped by 7,7,8,8 tetracyanoquinodimethane (TCNQ) due to the LUMO level of TCNQ is much higher than the HOMO of P3HT and the DOS has no overlaps [62,68]. P3HT doped by DDB-based dopants with low-lying LUMO level shows stronger polaron absorption than that of F4TCNQ-doped P3HT [48]. Gabriele *et al.* have found that the EA of F4TCNQ is sensitive to the position of dopant in the polymer network. EA of F4TCNQ is higher when it inserts in the alkyl chain region than that of in the π-conjugated backbone region, resulting in the formation of a large proportion of ICT [44]. Furthermore, it was found that the presence of dipole in dopant is also a considerable factor to affect the oxidization ability of dopants [62]. The ionization ratio and carrier concentration of 2-fluoro-7,7,8,8-tetracyanoquinodimethane (FTCNQ)-doped P3HT are far larger than the calculated values. It was proved that the DOS of FTCNQ is broadened due to the permanent dipole in FTCNQ molecule. That indicates the asymmetrical polar dopants are pre-

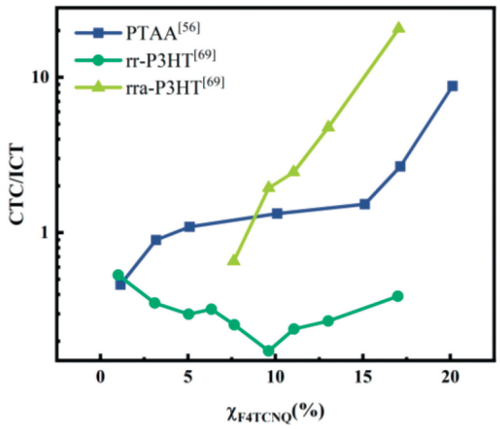

Fig. 7. The relationship between doping concentration and the ratio of CTC/ICT in F4TCNQ doped PTAA, rr-P3HT and rra-P3HT. Reproduced with permission [56]. Copyright 2021, American Chemical Society. Reproduced with permission [69]. Copyright 2018, American Chemical Society.

ferred to achieve more ICT. Therefore, using a substituted boron cluster as dopants leads P3HT to achieve a doping efficiency of about 100% due to a core-localized electron density [29].

4.2. Effect of microstructure on the degree of charge transfer

Optimization the microstructure by altering temperature, solvent, and doping method has been an effective way to control the degree of charge transfer.

Different local conformations of polymers upon doping have a significant impact on the charge transfer mechanism [41,54,69]. It was wildly accepted that ordered microstructure is inclined to produce ICT, while disordered microstructure will promote the formation of CTC. For instance, it is found that the proportion of CTC in rra-P3HT is much higher than that of rr-P3HT, because the disordered microstructure in the former film. Therefore, maintaining the ordered packing of polymers after doping is crucial for the formation of ICT. That means the low dopant concentration is needed to improve the degree of the charge transfer [16,54]. For example, if the doping concentration of F4TCNQ is less than 5%, ICT is the main mode of charge transfer in doped P3HT and poly[bis(4-phenyl) (2,4,6-trimethyl-phenyl)amine] (PTAA) (Fig. 7). With the increase of doping concentration, the proportion of CTC increases, and the conductivity decreases. Therefore, reducing the doping concentration of the disordered polymers can suppress the content of CTC and raise the proportion of ICT, thus increasing the doping efficiency [56,69].

Thermal annealing allows the rearrangement of conjugated backbone [70], which becomes a possible way to control the degree of the charge transfer. For example, the lamellar and π-stacking distance of P3HT linearly increase with increasing the substrate temperature [45,71], accompanying with dopant diffusion into the side chain and then the degree of charge transfer can be improved. The dopant moves from the π-stacking into the side chain region and CTC transforms into ICT after heating at 80 °C for 1 min. These results illustrate that the appropriate thermal annealing temperature and time can effectively reduce the proportion of CTC. Nevertheless, the high temperature probably causes the dedoping of the film due to the sublimation of the dopants. For example, it is found that the proportion of ICT decreases in F4TCNQ doped P3HT and PBTTT annealed at 70-120 °C for 20 min [45].

Besides, the choice of solvent during dissolving the polymer is another approach to improve the proportion of ICT. For example, blending chloroform with dichloromethane to dissolve P3HT can minimize chain movement so that dopants easily enter into

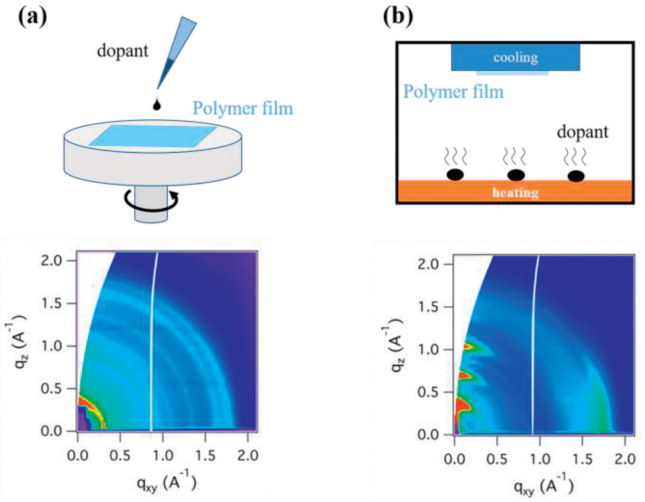

Fig. 8. (a) Solution-phase deposition and 2D GIWAXS images of P3HT solution doped F4TCNQ film. (b) Vapor-phase deposition and 2D GIWAXS images of P3HT vapor doped F4TCNQ film. Copied with permission [71]. Copyright 2018, American Chemical Society.

the side chain region to form ICT instead entering into π-stacking layers to form CTC [50]. Moreover, different doping methods also significantly affect the degree of charge transfer. Studies have revealed that less structure damage is induced in F4TCNQ vapor-doped P3HT films than the films prepared by mixing the polymer and dopant into a single solution (Fig. 8) [71], hence the higher the proportion of ICT is obtained in the former films [51].

4.3. Improved the doping efficiency by ion-exchange doping

The ion-exchange doping is first proposed by Shun Watanabe [72] to achieve higher efficient molecular doping. In the ion-exchange doping, the charge transfer occurs between conjugated polymer PBTTT and molecular dopants F4TCNQ. Then the F4TCNQ radical anions are replaced by anions of the ionic liquid. The transfer efficiency of F4TCNQ anions to ionic liquid anions is up to 98%, indicating the improved doping efficiency. Moreover, the ion-exchange doping efficiency is correlated to the strength of the ionic interaction, which is similar with the molecular doping process. More precisely, the low electrostatic surface potential of anion is needed. Although the conductivity is weakly dependent on the size of counterion [73], using a large polymer cation can reduce the diffusion of cation into solid film [74]. The selection of polymer for ionic exchange also has a great influence in the doping efficiency. For example, the D-A polymer poly[3-(2,2-bithien-5-yl)-2,5-bis(2-hexyldecyl)-2,5-dihydropyrrolo-[3,4-*c*]pyrrole-1,4-dione-6,5-diyl] (PDPP-2T) has achieved higher doping level than that of P3HT by ion-exchange doping by using $FeCl_3$ as dopant and $TFSI^-$ as ionic liquid anion [75]. In the ion-exchange doping, only integer charge transfer is considered and the redox potential limitation can be overcome [76]. In addition, the ordered microstructure can be maintained after ion-exchange doping due to the primary dopant anions are exchanged by the anions of ionic liquid which insert into the lamellar position. Thus, the increased ion intercalation and the polaron delocalization leads to the backbone planarization [77,78].

5. Summary and outlooks

As the chemical doping has become a widely used strategy to adjust the electrical performance of film devices, a fundamental and in-depth understanding of the charge transfer mechanism be-

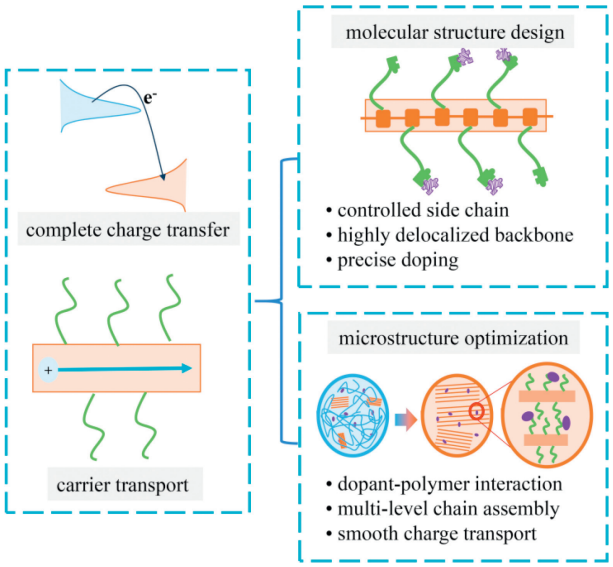

Fig. 9. Strategies and prospects for high-conductivity polymers.

tween OSC and dopant is essential. Although two kinds of mechanisms, ICT and CTC, have been proposed and widely accepted, the relationships between the charge transfer degree and the chemical structures, the molecular conformations and doping methodologies are still ambiguous. This review summarizes the basic characters of two mechanisms, discusses the key factors to affect the charge transfer degree, and finally introduces the strategies to increase the proportion of ICT through rational materials design and proper doping techniques.

There are still problems need to be developed. On one hand, how to improve doping efficiency and convert the localized charges into free carriers by precisely controlling charge transfer process remain big challenges. From the view of the materials structure, the design principle for ICT formation is not clear. How the conformation and relative position of polymer semiconductor and the dopants in solid state determine the number of the free carriers derived from ICT is still unknown. On the other hand, the charge transport mechanism related to the charge transfer is less reported so far. The holes seem to be trapped even for ICT species in which the Coulomb interaction plays a key role or not. Since appreciable dielectric constant screens mutual interaction in inorganic semiconductors, the dielectric constant of the OSC may be another factor need to be considered for the effective separation of holes and the corresponding anions.

Despite the existence of the forementioned challenges, the research about doping mechanism has been given intensive attention now as doping approaches have widely used in electronic devices. It can be foreseen that significant progress will be achieved with the help of a better understanding of molecular-structure relationship (Fig. 9), the advances of organic synthesis, and the better comprehension of the relevant transport physics.

Declaration of competing interest

The authors declare that they have no known competing financial interests or personal relationships that could have appeared to influence the work reported in this paper.

Acknowledgments

This work was supported by the National Natural Science Foundation of China (No. 92263109), the Shanghai Rising-Star Program (No. 22QA1410400) and Natural Science Foundation of Shanghai (No. 23ZR1472200).

References

[1] B.M.K. Walzer, M. Pfeiffer, K. Leo, Chem. Rev. 107 (2007) 1233–1271.
[2] Y. Zhao, W. Wang, Z. He, et al., Chin. Chem. Lett. 34 (2023) 108094.
[3] C.K. Chiang, C.R. Fincher, Y.W. Park, et al., Phys. Rev. Lett. 39 (1977) 1098–1101.
[4] Y. Yamamoto, K. Yoshino, Y. Inuishi, J. Phys. Soc. Jpn. 47 (1979) 1887–1891.
[5] R. Li, G. Xing, H. Li, et al., Chin. Chem. Lett. 34 (2023) 107454.
[6] R. Warren, A. Privitera, P. Kaienburg, et al., Nat. Commun. 10 (2019) 5538.
[7] A. Nollau, M. Pfeiffer, T. Fritz, et al., J. Appl. Phys. 87 (2000) 4340–4343.
[8] R.Q. Png, M.C. Ang, M.H. Teo, et al., Nat. Commun. 7 (2016) 11948.
[9] A.F. Paterson, Y.H. Lin, A.D. Mottram, et al., Adv. Electron. Mater. 4 (2018) 1700464.
[10] X. Dai, L. Liu, Z. Ji, et al., Chin. Chem. Lett. 34 (2023) 107239.
[11] M. Koopmans, M.A.T. Leiviska, J. Liu, et al., ACS Appl. Mater. Interfaces 12 (2020) 56222–56230.
[12] F. Ghani, A. Opitz, P. Pingel, et al., J. Polym. Sci. B 53 (2015) 58–63.
[13] S.N. Patel, A.M. Glaudell, K.A. Peterson, et al., Sci. Adv. 3 (2017) e1700434.
[14] B.Z. Li, X.X. Li, F. Yang, et al., ACS Appl. Energy Mater. 4 (2021) 4662–4671.
[15] H. Li, M.E. DeCoster, R.M. Ireland, et al., J. Am. Chem. Soc. 139 (2017) 11149–11157.
[16] H. Li, Z. Xu, J. Song, et al., Adv. Funct. Mater. 32 (2021) 2110047.
[17] A.F. Paterson, R. Li, A. Markina, et al., J. Mater. Chem. C 9 (2021) 4486–4495.
[18] K. Kang, S. Watanabe, K. Broch, et al., Nat. Mater. 15 (2016) 896–902.
[19] I.E. Jacobs, E.W. Aasen, J.L. Oliveira, et al., J. Mater. Chem. C 4 (2016) 3454–3466.
[20] H. Yan, Y. Tang, X. Meng, et al., ACS Appl. Mater. Interfaces 11 (2019) 4178–4184.
[21] H. Zhang, X. Zhang, Y. Li, et al., Sol. RRL 6 (2022) 2101096.
[22] S.E. Yoon, Y. Kang, S.Y. Noh, et al., ACS Appl. Mater. Interfaces 12 (2020) 1151–1158.
[23] A.M. Glaudell, J.E. Cochran, S.N. Patel, et al., Adv. Energy Mater. 5 (2015) 1401072.
[24] H. Chai, Z. Xu, H. Li, et al., ACS Appl. Electron. Mater. 4 (2022) 4947–4954.
[25] E.M. Thomas, K.A. Peterson, A.H. Balzer, et al., Adv. Electron. Mater. 6 (2020) 2000595.
[26] S.E. Yoon, Y. Kang, G.G. Jeon, et al., Adv. Funct. Mater. 30 (2020) 2004598.
[27] P. Li, X. Ai, Q. Zhang, et al., Chin. Chem. Lett. 32 (2021) 811–815.
[28] P. Pingel, D. Neher, Phys. Rev. B 87 (2013) 035502.
[29] T.J. Aubry, J.C. Axtell, V.M. Basile, et al., Adv. Mater. 31 (2019) e1805647.
[30] T. Ma, B.X. Dong, J.W. Onorato, et al., J. Polym. Sci. 59 (2021) 2797–2808.
[31] M.L. Tietze, J. Benduhn, P. Pahner, et al., Nat. Commun. 9 (2018) 1182.
[32] I. Salzmann, G. Heimel, S. Duhm, et al., Phys. Rev. Lett. 108 (2012) 035502.
[33] W.B.P. Robert, S. Mulliken, J. Am. Chem. Soc. 91 (1969) 3409–3413.
[34] M.J. Mantione, Theor. Chem. Acc. 11 (1968) 119–127.
[35] D.T. Duong, C. Wang, E. Antono, et al., Org. Electron. 14 (2013) 1330–1336.
[36] H. Mendez, G. Heimel, A. Opitz, et al., Angew. Chem. Int. Ed. 52 (2013) 7751–7755.
[37] I. Salzmann, G. Heimel, J. Electron. Spectrosc. Relat. Phenomena 204 (2015) 208–222.
[38] I. Salzmann, G. Heimel, M. Oehzelt, et al., Acc. Chem. Res. 49 (2016) 370–378.
[39] C. Wang, D.T. Duong, K. Vandewal, et al., Phys. Rev. B 91 (2015) 085205.
[40] M.P. Gordon, S.A. Gregory, J.P. Wooding, et al., Appl. Phys. Lett. 118 (2021) 233301.
[41] I.E. Jacobs, C. Cendra, T.F. Harrelson, et al., Mater. Horiz. 5 (2018) 655–660.
[42] K.E. Watts, B. Neelamraju, E.L. Ratcliff, et al., Chem. Mater. 31 (2019) 6986–6994.
[43] E. Kampar, O. Neilands, Russ. Chem. Rev. 55 (1986) 637–651.
[44] M. Comin, V. Lemaur, A. Giunchi, et al., J. Mater. Chem. C 10 (2022) 13815–13825.
[45] O. Zapata-Arteaga, B. Dorling, A. Perevedentsev, et al., Macromolecules 53 (2020) 609–620.
[46] V. Untilova, T. Biskup, L. Biniek, et al., Macromolecules 53 (2020) 2441–2453.
[47] H. Hase, K. O'Neill, J. Frisch, et al., J. Phys. Chem. C 122 (2018) 25893–25899.
[48] T.J. Aubry, K.J. Winchell, C.Z. Salamat, et al., Adv. Funct. Mater. 30 (2020) 2001800.
[49] E.M. Thomas, E.C. Davidson, R. Katsumata, et al., ACS Macro Lett. 7 (2018) 1492–1497.
[50] D.A. Stanfield, Y. Wu, S.H. Tolbert, et al., Chem. Mater. 33 (2021) 2343–2356.
[51] E.C. Wu, C.Z. Salamat, S.H. Tolbert, et al., ACS Appl. Mater. Interfaces 14 (2022) 26988–27001.
[52] E.F. Aziz, A. Vollmer, S. Eisebitt, et al., Adv. Mater. 19 (2007) 3257–3260.
[53] H. Wu, Y. Sun, L. Sun, et al., Chin. Chem. Lett. 32 (2021) 3007–3010.
[54] H. Méndez, G. Heimel, S. Winkler, et al., Nat. Commun. 6 (2015) 8560.
[55] C.D. Dong, S. Schumacher, J. Phys. Chem. C 123 (2019) 30863–30870.
[56] M. Cui, H. Rui, X. Wu, et al., J. Phys. Chem. Lett. 12 (2021) 8533–8540.
[57] Z.Y. Wang, J.Y. Wang, J. Pei, Chin. Chem. Lett. 30 (2019) 25–30.
[58] R. Ghosh, A.R. Chew, J. Onorato, et al., J. Phys. Chem. C 122 (2018) 18048–18060.
[59] M. Heydari Gharahcheshmeh, K.K. Gleason, Mater. Today Adv. 8 (2020) 100086.
[60] L. Wang, C. Pan, Z. Chen, et al., Polym. Chem. 9 (2018) 4440–4447.
[61] S.J. Yoo, J.J. Kim, Macromol. Rapid Commun. 36 (2015) 984–1000.

[62] H. Hase, M. Berteau-Rainville, S. Charoughchi, et al., Appl. Phys. Lett. 118 (2021) 203301.
[63] D. Kiefer, R. Kroon, A.I. Hofmann, et al., Nat. Mater. 18 (2019) 149–155.
[64] P. Durand, H.Y. Zeng, T. Biskup, et al., Adv. Energy Mater. 12 (2022) 2103049.
[65] C. Cui, W.Y. Wong, Macromol. Rapid Commun. 37 (2016) 287–302.
[66] J. Yang, Y. Li, S. Duhm, et al., Adv. Mater. Interfaces 1 (2014) 1300128.
[67] J.T. Liu, H. Hase, S. Taylor, et al., Angew. Chem. Int. Ed. 59 (2020) 7146–7153.
[68] P.Y. Yee, D.T. Scholes, B.J. Schwartz, et al., J. Phys. Chem. Lett. 10 (2019) 4929–4934.
[69] B. Neelamraju, K.E. Watts, J.E. Pemberton, et al., J. Phys. Chem. Lett. 9 (2018) 6871–6877.
[70] N. Sun, H. Gao, L. Sun, et al., Chin. Chem. Lett. 33 (2022) 835–841.
[71] E. Lim, K.A. Peterson, G.M. Su, et al., Chem. Mater. 30 (2018) 998–1010.
[72] Y. Yamashita, J. Tsurumi, M. Ohno, et al., Nature 572 (2019) 634–638.
[73] C. Chen, I.E. Jacobs, K. Kang, et al., Adv. Energy Mater. 13 (2023) 2202797.
[74] D. Yuan, E. Plunkett, P.H. Nguyen, et al., Adv. Funct. Mater. 33 (2023) 2300934.
[75] T.L. Murrey, M.A. Riley, G. Gonel, et al., J. Phys. Chem. Lett. 12 (2021) 1284–1289.
[76] S.E. Yoon, J. Park, J.E. Kwon, et al., Adv. Mater. 32 (2020) e2005129.
[77] I.E. Jacobs, Y. Lin, Y. Huang, et al., Adv. Mater. 34 (2022) e2102988.
[78] Y. Yamashita, J. Tsurumi, T. Kurosawa, et al., Commun. Mater. 2 (2021) 45.